

SANDIA REPORT

SAND2019-4962

Printed May 2019



Sandia
National
Laboratories

Big Hill 2018 InSAR Analysis, U.S. Strategic Petroleum Reserve

Anna S. Lord

Prepared by
Sandia National Laboratories
Albuquerque, New Mexico
87185 and Livermore,
California 94550

Issued by Sandia National Laboratories, operated for the United States Department of Energy by National Technology & Engineering Solutions of Sandia, LLC.

NOTICE: This report was prepared as an account of work sponsored by an agency of the United States Government. Neither the United States Government, nor any agency thereof, nor any of their employees, nor any of their contractors, subcontractors, or their employees, make any warranty, express or implied, or assume any legal liability or responsibility for the accuracy, completeness, or usefulness of any information, apparatus, product, or process disclosed, or represent that its use would not infringe privately owned rights. Reference herein to any specific commercial product, process, or service by trade name, trademark, manufacturer, or otherwise, does not necessarily constitute or imply its endorsement, recommendation, or favoring by the United States Government, any agency thereof, or any of their contractors or subcontractors. The views and opinions expressed herein do not necessarily state or reflect those of the United States Government, any agency thereof, or any of their contractors.

Printed in the United States of America. This report has been reproduced directly from the best available copy.

Available to DOE and DOE contractors from

U.S. Department of Energy
Office of Scientific and Technical Information
P.O. Box 62
Oak Ridge, TN 37831

Telephone: (865) 576-8401
Facsimile: (865) 576-5728
E-Mail: reports@osti.gov
Online ordering: <http://www.osti.gov/scitech>

Available to the public from

U.S. Department of Commerce
National Technical Information Service
5301 Shawnee Rd
Alexandria, VA 22312

Telephone: (800) 553-6847
Facsimile: (703) 605-6900
E-Mail: orders@ntis.gov
Online order: <https://classic.ntis.gov/help/order-methods/>



ABSTRACT

The historical subsidence surveys shot over the U.S. Strategic Petroleum Reserve Big Hill site, located in southeastern Texas, have indicated surface uplift since 2002. In order to better understand and substantiate the surface behavior inferred from annual elevation measurements, InSAR (interferometric synthetic aperture radar) data was acquired. InSAR involves the processing of multiple satellite synthetic aperture radar scenes acquired across the same location of the Earth's surface at different times to map surface deformation. The analysis of the data can detect millimeters of motion spanning days, months, year and decades, across specific sites.

The InSAR analysis indicates the fastest subsidence rates are over the north central region of the site, specifically centered over caverns 104 and 103. Subsidence rates decrease towards both the west and east, with the western side subsiding at greater rate than the eastern edge. There is some uplift noted, off the site and off the dome to the east. Overall, the subsidence pattern is in line with subsidence behavior expected over a cavern field.

In investigating the validity of the uplift measured during the ground surveys it was discovered that reference location can impact results. An exercise was conducted that took the current InSAR data and presented two varying results dependent on the reference location, either on or off the dome. The conclusion was that if the reference is located on the dome, as it has been for years for the ground surveys, the reference location is moving too, giving the appearance of uplift.

CONTENTS

| | |
|--|------------------------------|
| 1. Introduction | 10 |
| 2. Geology | 12 |
| 3. Ground Survey | 15 |
| 4. InSAR | 19 |
| 4.1. Historic InSAR Analysis | 19 |
| 4.2. Current InSAR Analysis | 22 |
| 4.2.1. Line of Sight Results | 23 |
| 4.2.2. 2D Results | 24 |
| 4.2.2.1. Vertical Surface Displacement | 24 |
| 4.2.2.2. Horizontal Surface Displacement | 30 |
| 5. Discussion | 32 |
| Appendix A. Main Appendix Title..... | Error! Bookmark not defined. |
| A.1. Sub-Appendix Title..... | Error! Bookmark not defined. |

LIST OF FIGURES

| | |
|---|----|
| Figure 1. Map of Texas, Louisiana, and Mississippi showing the locations of the four SPR sites..... | 11 |
| Figure 2. 2005 Big Hill top-of-caprock and top-of-salt structure contour maps..... | 13 |
| Figure 3. Top-of-caprock structure contour map with fault interpretation by Neal and others, 1993..... | 14 |
| Figure 4. Total subsidence at the Big Hill SPR site beginning in January 2002, when 135 new monuments were added to the site. The approximate location of BH-109 (red circle) is shown for reference. (Figure 4, from Moriarty 2017)..... | 16 |
| Figure 5. Total subsidence at the Big Hill site between January 2002 and July 2017. | 17 |
| Figure 6. Locations of benchmarks in reference to the Big Hill SPR site with white benchmarks used for surveys leading up to 2017 and the blue benchmarks used for all future surveys. (Figure 6, from Moriarty 2018)..... | 18 |
| Figure 7. Temporal distribution | 19 |
| Figure 8. ALOS imagery. Mean displacement rate (mm/yr) across Big Hill for 2007-2022. From Figure 10, CGG 2014) | 21 |
| Figure 9. Averaged displacement time-series across the Big Hill site for 2007-2011. (From Figure 11, CGG 2014)..... | 22 |
| Figure 10. Time period covered by satellite data sets..... | 23 |
| Figure 11. Annual surface displacement rates obtained from the ascending and descending LOS analysis..... | 24 |
| Figure 12. Surface displacement results obtained from the vertical analysis..... | 25 |
| Figure 13. Vertical deformation rate with six areas highlighted for average time series. | 26 |
| Figure 14. Average time series of the six areas highlight in Figure 13. | 27 |
| Figure 15. Trace of the cross-section lines over the salt dome. Vertical cross sections are shown in Figure 16 to Figure 18. | 28 |
| Figure 16. Evolution of the surface profile cross section A – A'. The solid profile highlighted in red corresponds to the final image of the data stack. The dashed vertical line in red corresponds to the location on the profile line where the elevation of salt changes (1650-feet). | 29 |
| Figure 17. Evolution of the surface profile cross section B – B'. The solid profile highlighted in red corresponds to the final image of the data stack. The contrasting background colors (pink/green) illustrate where the profile crosses the 4000-ft salt contour, while the dashed vertical line in red corresponds to the edge of the salt dome on the profile line. | 29 |

| | |
|---|----|
| <i>Figure 18. Evolution of the surface profile cross section C – C' in Figure 13. The solid profile highlighted in red corresponds to the final image of the data stack. The contrasting background colors (pink/green) illustrate where the profile crosses the 4000-ft salt contour, while the dashed vertical lines in red corresponds to the edge of the salt dome on the profile line.</i> | 30 |
| <i>Figure 19</i> | 31 |
| <i>Figure 20. Comparison of deformation rates obtained from the ascending InSAR results and ground-based surveys. Top left: Deformation rates obtained from the ascending InSAR analysis; Bottom right: Deformation rates calculated from ground-based survey measurements projected to satellite's LOS. Note that the network's reference point exhibits subsidence within InSAR results; Bottom left: Deformation rates obtained from the ascending InSAR analysis using a reference with known subsidence issues.</i> | 33 |
| <i>Figure 21. Big Hill subsidence rates, January 2018 to January 2109.</i> | 34 |

LIST OF TABLES

| | |
|---|----|
| <i>Table 1. InSAR data sets</i> | 20 |
| <i>Table 2. 2-D InSAR data sets</i> | 23 |

This page left blank

ACRONYMS AND DEFINITIONS

| Abbreviation | Definition |
|--------------|--|
| InSAR | interferometric synthetic aperture radar |
| SPR | Strategic Petroleum Reserve |

1. INTRODUCTION

The U.S. Strategic Petroleum Reserve (SPR) is a stockpile of emergency crude oil to be tapped into if a disruption in the nation's oil supply occurs. The SPR comprises of four salt dome sites located within Texas and Louisiana (Figure 1). Subsidence surveys have been conducted either annually or biennially at all four sites over the life of the program. Monitoring of surface behavior is a first line defense to detecting possible subsurface cavern integrity issues. In recent years the SPR Big Hill site, located in southeastern Texas, has experienced a host of well failures. In conjunction the subsidence surveys have indicated surface uplift predominantly along the eastern perimeter and to a lesser extent along the western perimeter of the site. Over the center of the field there has been a general decrease in subsidence rate over time.

Big Hill subsidence surveys began in 1989 with only 38 monuments being measured, with 28 of those being well heads. In 2002, 135 monuments were added which improved coverage and extended the monitoring beyond the caverns to both the east and west of the field. Surface uplift was first noted after the addition of the 135 monuments. Since 2002, Big Hill subsidence trends have indicated continuous surface uplift towards the eastern region of the site, whereas subsidence, though minor, has continued to occur across the rest of the site [1, 2, 3,4].

In order to better understand and substantiate the surface behavior inferred from annual elevation measurements, InSAR (interferometric synthetic aperture radar) data was acquired. InSAR involves the processing of multiple satellite synthetic aperture radar scenes acquired across the same location of the Earth's surface at different times to map surface deformation. The analysis of the data can detect millimeters of motion spanning days, months, year and decades, across specific sites. This report describes the InSAR analysis results, how those results compare to the historical collection of land survey data, and what additional information the data has provided towards identifying the source causing the response recorded at the surface.



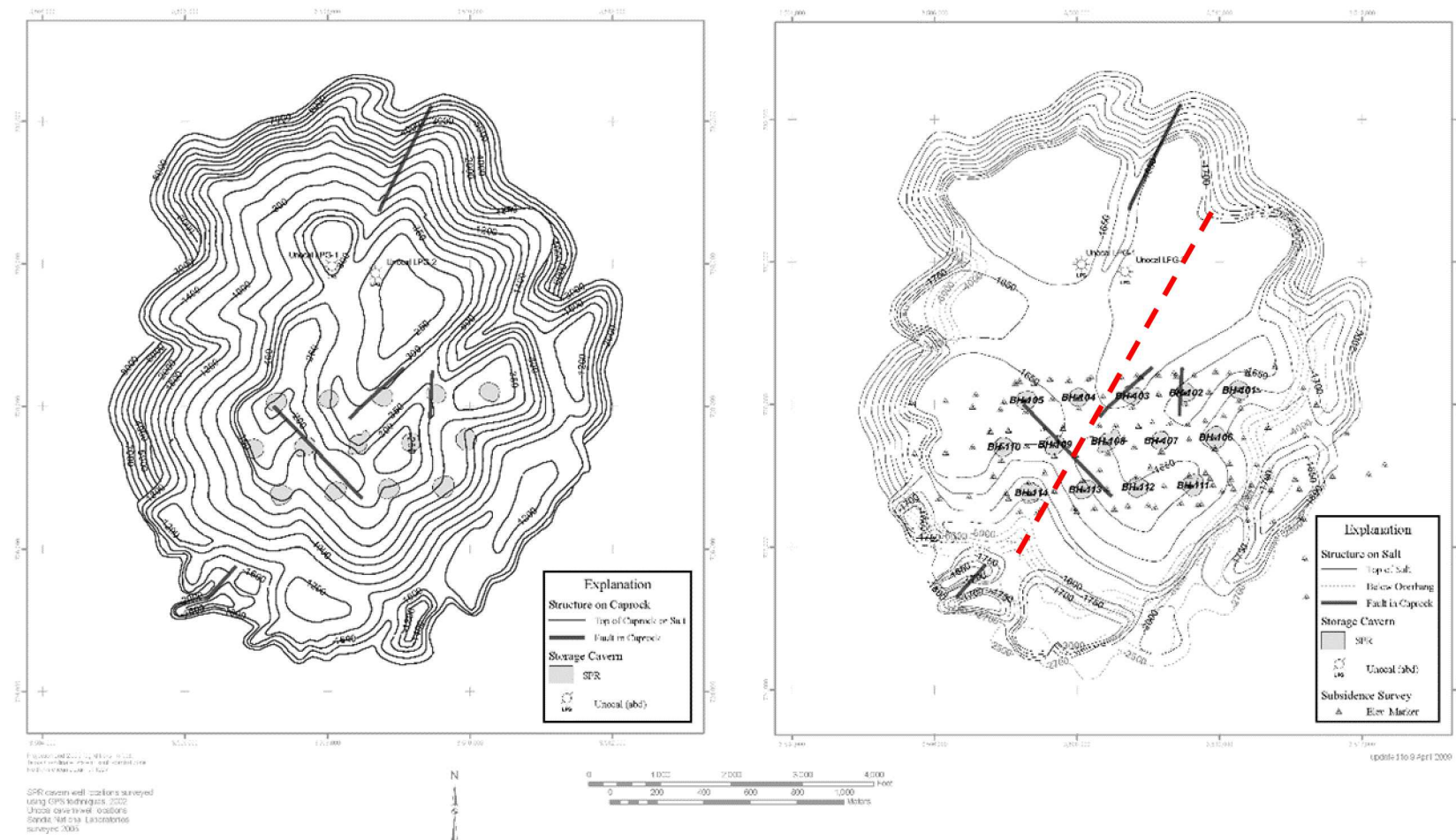
Figure 1. Map of Texas, Louisiana, and Mississippi showing the locations of the four SPR sites.

2. GEOLOGY

The Big Hill salt dome is generally cylindrical in shape and leans towards the south with the top of salt being relatively flat at a depth at approximately 1600 feet (Figure 2). The flanks are not smooth, but rather exhibit a crenulated fabric. The salt overhangs largely to the south with less prominent overhangs present along both the western and eastern sides of the salt flanks.

At Big Hill the caprock comprises a lower anhydrite zone overlain by a limestone and gypsum zone, both of which are diagenetic alterations of anhydrite. The top of caprock is approximately 300 feet below surface. The caprock is unusually thick and ranges in thickness between 850 and 1300 feet in the SPR storage region. Lost circulation issues were encountered during drilling for cavern construction, and cores show that the caprock internal structure is very complicated. The caprock structure exhibits vugs, faults, and fractures, all of which were caused by dissolution of the underlying salt during dome growth and hence the collapse of the salt-caprock interface, resulting in a highly permeable caprock.

At Big Hill, salt spines, mapped by Magorian and Neal [5], appear as anticlinal features within the dome. A shear zone is interpreted to fall between caverns 104, 109, and 114, and caverns 103, 108, and 113 based on subsurface correlations (Figure 2). The shear zone correlates with the major fault mapped on top of the caprock by Neal and others [6] (Figure 3).



Geologic Structure of the Big Hill Salt Dome, Texas

Figure 2. 2005 Big Hill top-of-caprock and top-of-salt structure contour maps.

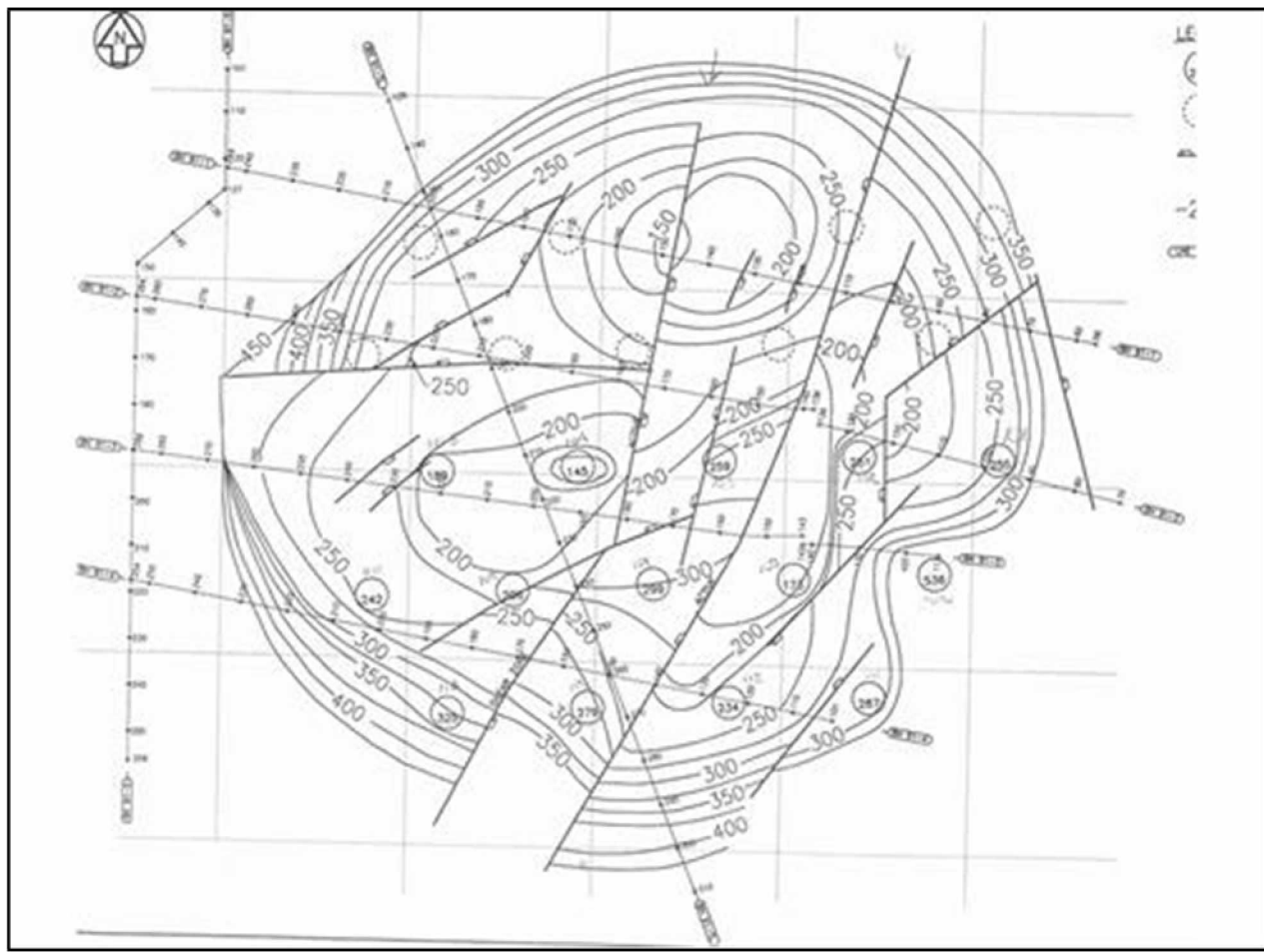


Figure 3. Top-of-caprock structure controu map with fault interpretation by Neal and others [6].

3. GROUND SURVEY

Subsidence surveys have been conducted annually or biennially since 1989 over the Big Hill site. Since 2002, with the addition of 135 new monuments, elevation measurements have indicated continuous surface uplift over the eastern edge of the site. Figure 4 and Figure 5 displays the historic subsidence trend noted since 2002. Note the warmer shades of color suggest uplift.

The recorded behavior is unusual, and all potential data were examined in an effort to explain the surface deformation pattern. The geology, cavern closure rates, and waste injection volumes to the south of the site, were all considered [4,7, 8, 9]. There was no clear contributor, but the unexpected subsidence pattern was postulated to be due to rigid body rotation of the massive caprock. This rotation was believed to result from faulting that creates caprock blocks which are tilted downward in the subsided region above the caverns and hinge up outside the cavern field.

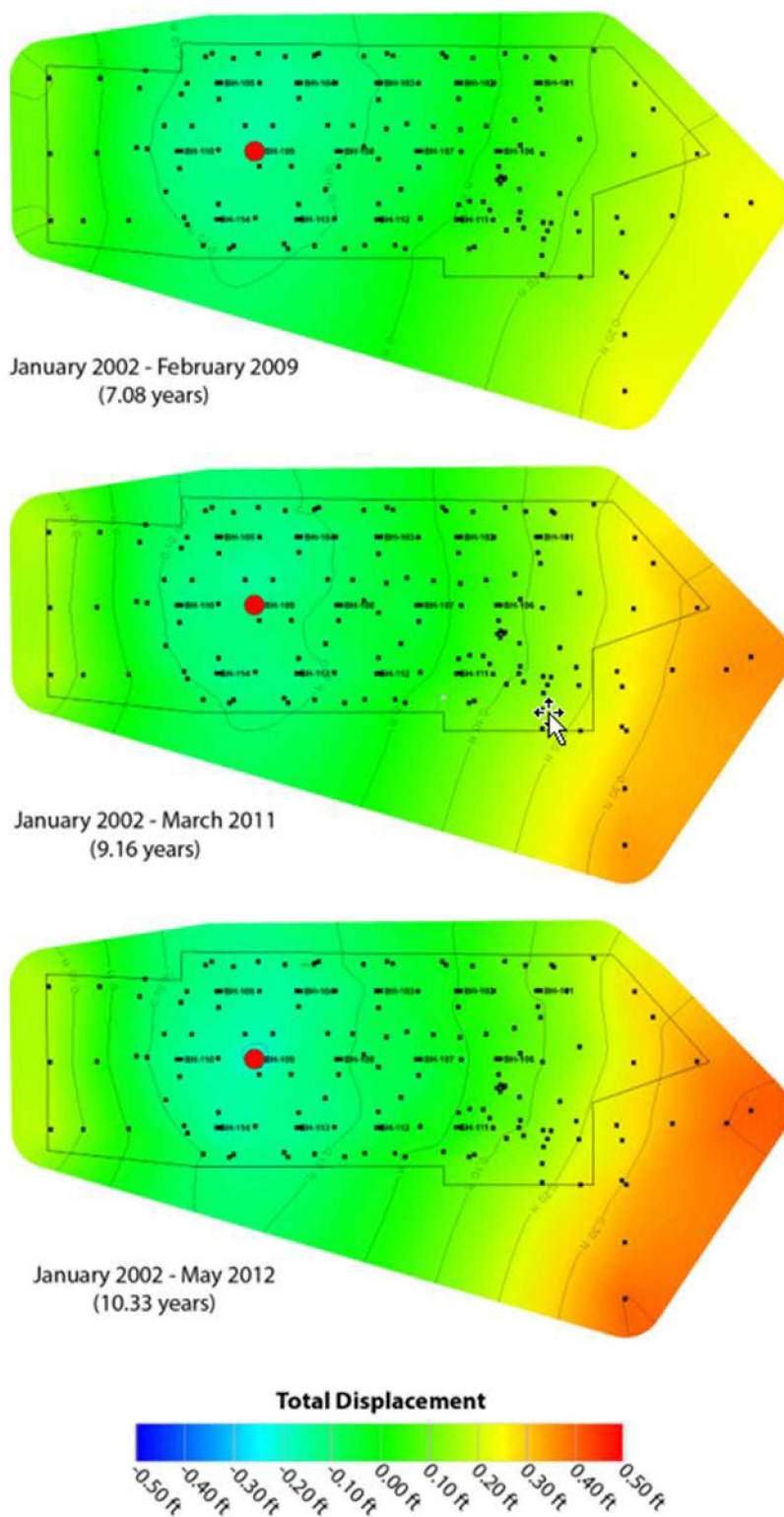


Figure 4. Total subsidence at the Big Hill SPR site beginning in January 2002, when 135 new monuments were added to the site. The approximate location of BH-109 (red circle) is shown for reference [10] (Figure 4).

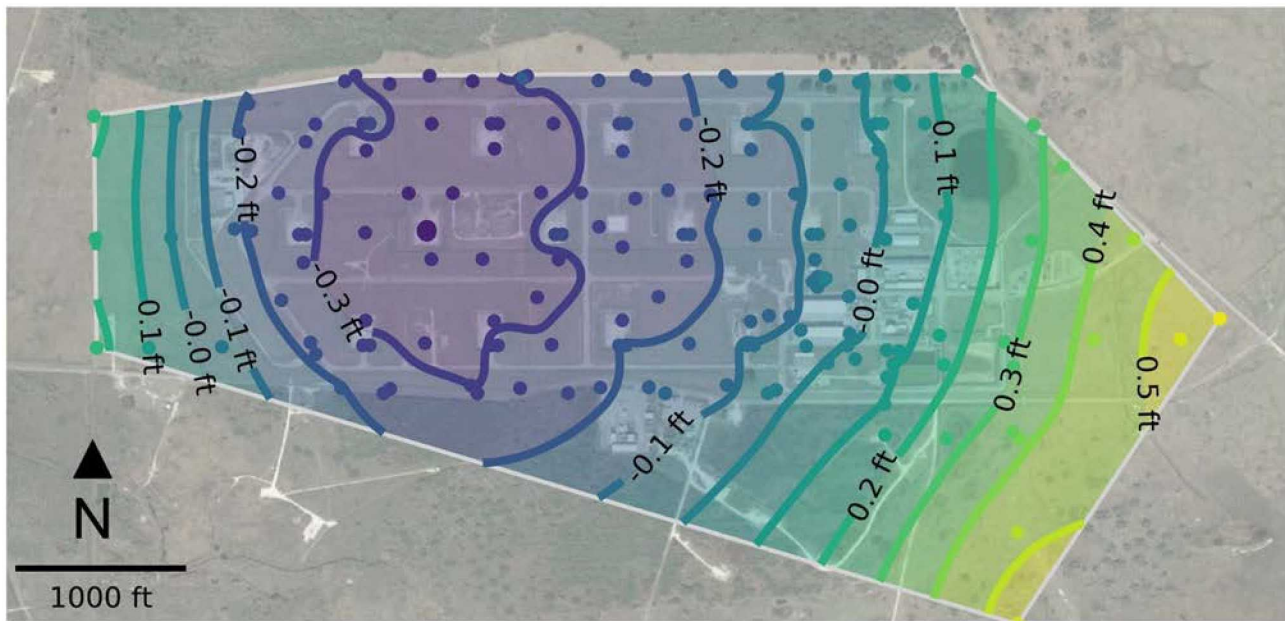


Figure 5. Total subsidence at the Big Hill site between January 2002 and July 2017.

All these surveys, were conducted, referencing a benchmark, located north of the site, on the dome. The surveys prior to 2018 survey were based on the datum just north of the site named Reidel 1931. There are two secondary monuments nearby named Reidel Reference Monument No. 2 and No. 4. The secondary locations were used if the primary datum could not be accessed or was damaged. In 2018 new reference locations were established off the dome. For the current and all future surveys, four benchmarks were established approximately 3.3 miles from the middle of the Big Hill site. The new reference monuments, named Big Hill No. 136-139, were referenced to Reidel No. 2. The approximate locations for all reference monuments in relation to the site are shown in Figure 6. Moving the reference location off the dome, should provide more independence from the dome behavior influence, thus improving the validity of the results.

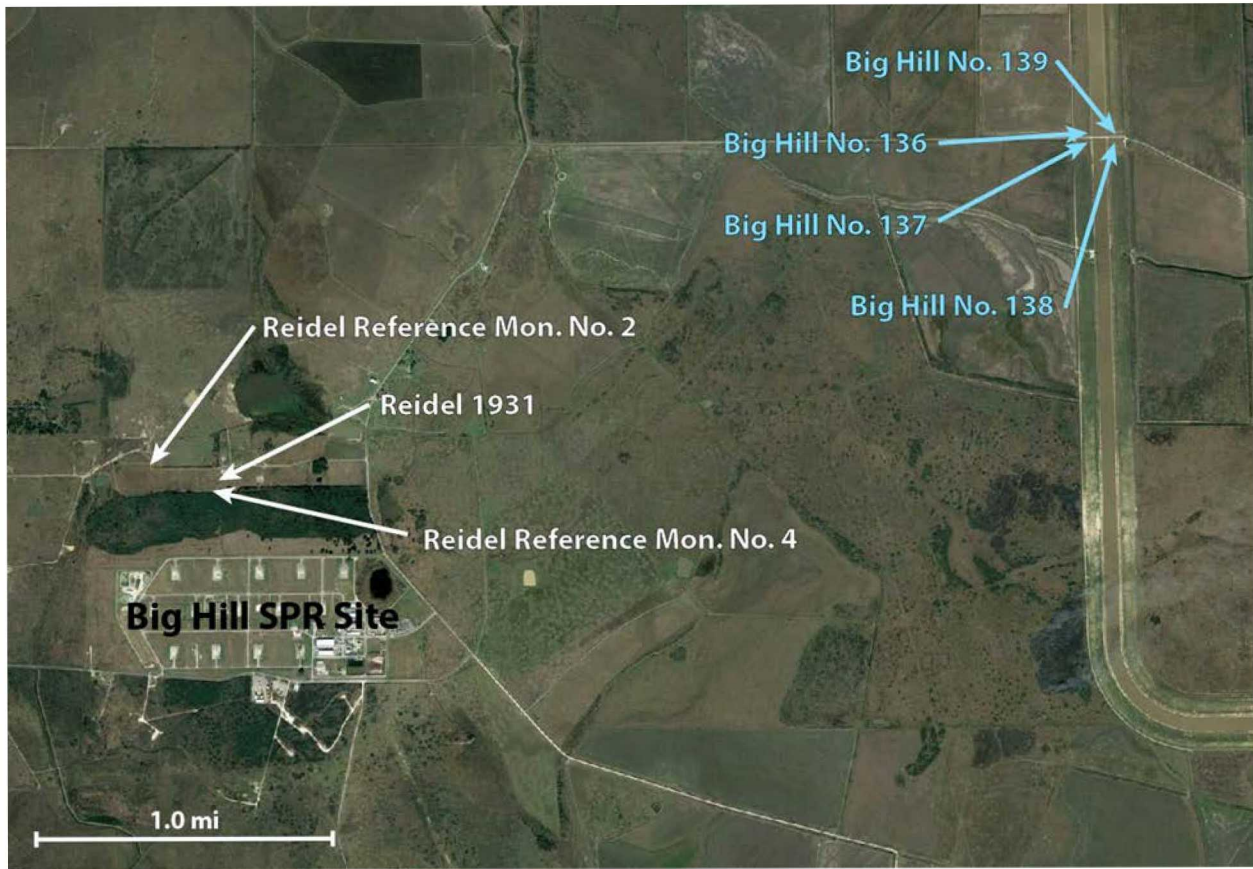


Figure 6. Locations of benchmarks in reference to the Big Hill SPR site with white benchmarks used for surveys leading up to 2017 and the blue benchmarks used for all future surveys [11] (Figure 6.)

4. INSAR

Interferometric synthetic aperture radar (InSAR) involves the processing of multiple satellite synthetic aperture radar scenes acquired across the same location of the Earth's surface at different times to map surface deformation. Analysis of the data can possibly detect millimeters of motion spanning days, months, year and decades, across specific sites. The intent in regard to the Big Hill site is (1) to substantiate the surface uplift trend recorded by land survey, (2) understand the regional surface behavior, and (3) possibly be able to understand the subsurface source impacting the ground deformation pattern. To date, two separate collections of InSAR data sets have been acquired, historic and real-time.

InSAR data results can be presented in a 1-D or 2-D format. InSAR measures surface displacement on a one-dimensional plane, along the satellite line-of-sight. Data can be collected from either ascending orbit or descending orbits. The line-of-sight angles can vary dependent on satellite location. Ascending satellites travel from south to north while imaging to the east, whereas descending satellites travel from north to south and image to the west. By combining results from the two acquisition geometries a true vertical displacement and east-west horizontal displacement can be derived, known as a two-dimensional (2D) movement analysis.

In 2014, the program purchased historic InSAR data that had been previously shot over the region that included the Big Hill site. Data obtained was not continuous but spanned over a time frame between 1992 and 2011. The imagery data are historic, which means that radar scenes were shot over the Big Hill area in the past. The acquired imagery data were not tailored for the project's purposes, but were acquired as part of the satellites' background scientific missions; hence the data imagery is rarely optimal, but collection of the available data provide a unique and relatively low-cost opportunity to detect historical deformation trends. This data can only be presented in a 1-D format.

Presently, Sandia has initiated a program collecting real-time InSAR imagery and received the first analysis in December 2018, which spans the time between September 2017 to September 2018. The collection of imagery was designed to capture radar scenes to meet the program's needs and to present the data in a 2-D format. InSAR imagery will continue to be collected over the current year through September 2019.

4.1. Historic InSAR Analysis

In 2014, historic interferometric synthetic aperture radar (InSAR) data was purchased and processed by CGG. The InSAR collected encompassed radar data from June 1992 to November 2000 and between January 2007 and January 2011. Note there is a data gap between 2000 and 2007. The data purchased were from the European Space Agency's (ESA) ERS-1/-2 satellites and from the Japanese Space Agency's (JAXA) ALOS satellite. Figure 7 and Table 1 display the temporal distribution of the data stacks. The references used in the analysis were located off dome in the city of Beaumont for the ERS satellite analysis and in the city of Winnie for the ALOS analysis.

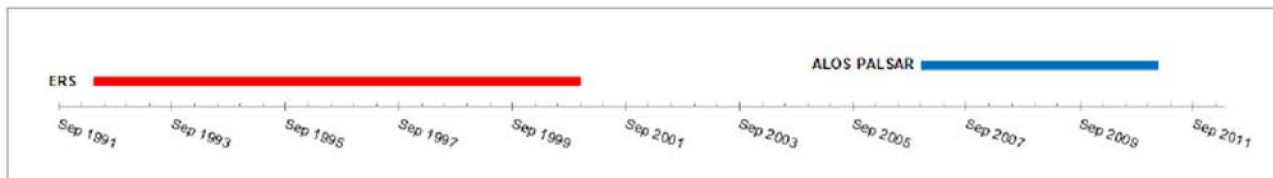


Figure 7. Temporal distribution of the acquired data stacks [12].

Table 1. InSAR data sets.

| Satellite | Geometry | No. of Images | Number of Measurement Points | Repeat Interval | Acquisition Period |
|-------------|------------|---------------|------------------------------|-----------------|-------------------------|
| ESA (ERS) | Descending | 24 | 242 | ~35 - days | 06/01/1992 - 11/30/2000 |
| JAXA (ALOS) | Ascending | 20 | 643 | ~45 - days | 01/05/2007 - 01/16/2011 |

The InSAR data analysis and interpretation were presented at the 2015 Solution Mining Research Institute Fall technical conference [7]. The ERS satellite data analyzed between 1992 and 2000 was sparse, but indicated the entire Big Hill region was subsiding during that time. The subsidence rate on average was -3.5 mm/yr. between 1992 and 2000. In comparison the average rate calculated between 1992 and 1999 using the ground survey data was -3.8 mm/yr. The average was calculated from measurements recorded at only the cavern wellheads. The rates compare well.

The ALOS data spans from 2007 – 2011. The ALOS satellite data uses a longer radar wavelength than the ERS satellite, which improves correlation through time. This along with the more regular acquisitions allowed for a greater density of data acquisition cross the Big Hill site. Figure 8 displays the results over the Big Hill site.

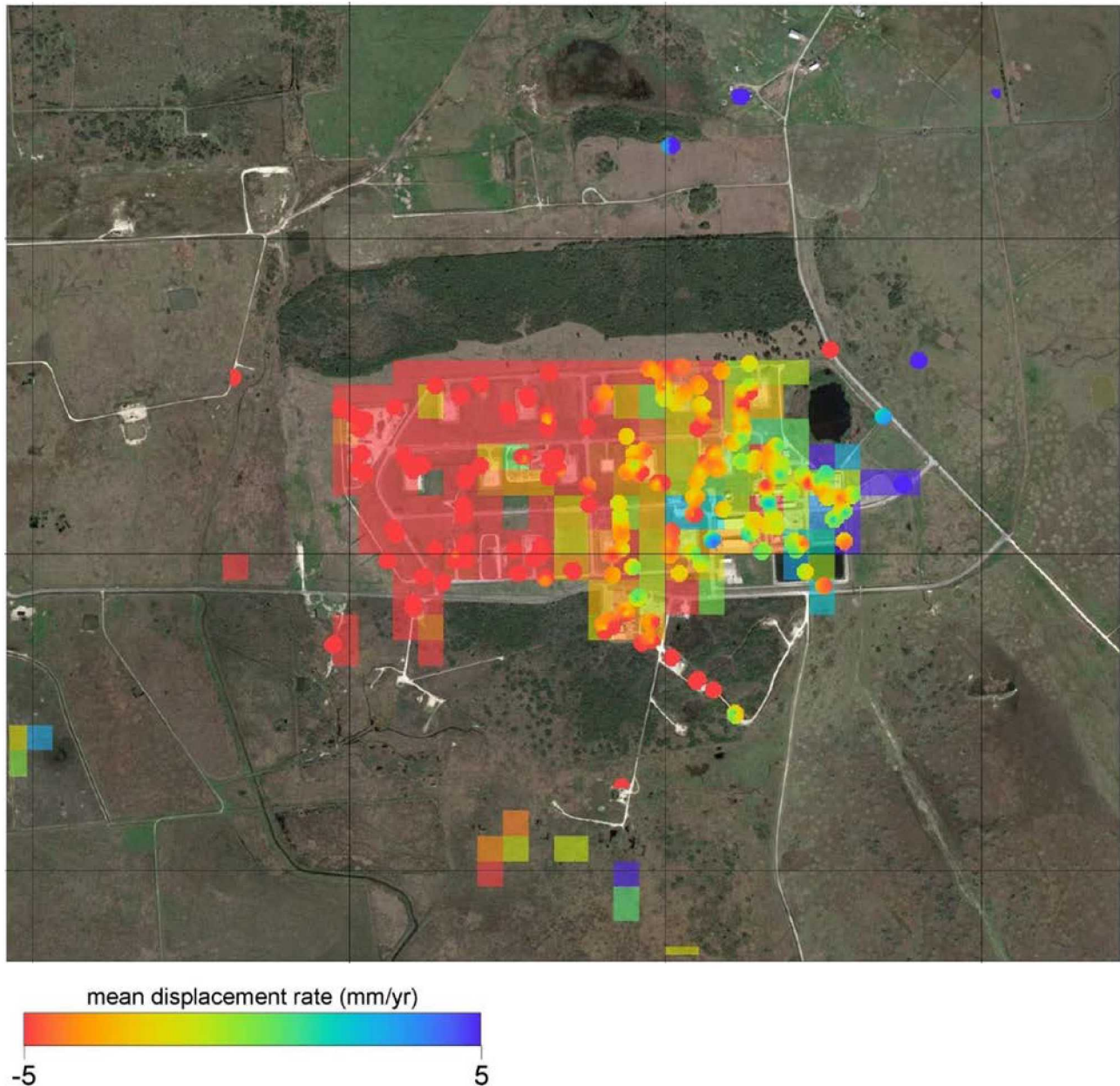


Figure 8. ALOS imagery. Mean displacement rate (mm/yr.) across Big Hill for 2007-2022 [12].

Subsidence rates were greatest across the western region of the site averaging between -7 and -9 mm/yr., with rates reducing eastward towards 0 mm/yr. along the eastern edge. A few points outside the property and mostly off the dome indicated uplift ranging between 5 and 10 mm/yr.

Figure 9 displays a time series of site wide averaged surface displacement rates. The plot displays that a shift in surface displacement rate occurred during 2009. Before 2009 the site was subsiding at approximately -7 mm/yr. and then subsidence slowed and essentially stops between 2009 and the end of the data set (January 2011).

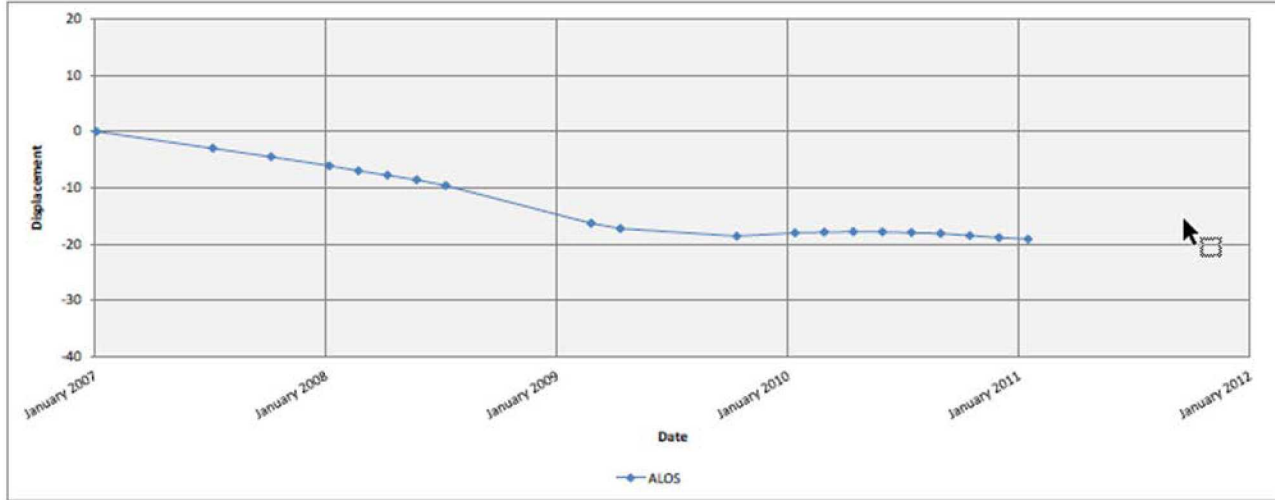


Figure 9. Averaged displacement time-series across the Big Hill site for 2007-2011 [12].

Lord, 2015 dived deeper into the data and analyzed a subset of time series parceled across the site from both west to east and north to south. The subset of time series plots from west to east inferred that subsidence is occurring over the western region of the site. The subsidence behavior then changes from a general subsiding trend to a gradual decrease in deformation rates around the location near the middle of the site. The decrease in deformation coincides, generally, with the area of the mapped caprock graben fault block (See Figure 3 above CR map). The subsidence rate over the eastern region of the site is nearly zero, with a few points measuring uplift. A subset of time series was also examined from the north to south inferring subsidence rates are highest in the north and decrease towards the south.

Only one ground survey occurred during the time encompassed by historic ALOS InSAR data. As such, comparisons are hard to make. The two sets of historic data acquired also do not cover the time around 2002 when our ground survey first recorded and inferred uplift at the site. It is important to note that these are two completely different data sets that were each designed differently, where one measures a region and the other a set of points and over different frequency intervals. InSAR data are collected at a higher frequency and may detect dynamic trends seen only over a short time frame or within a small region with more data coverage than the ground surveys can provide. In addition, the reference point differs between the two techniques. However, both data sets inferred uplift is occurring and predominantly over the eastern region of the site.

4.2. Current InSAR Analysis

InSAR data results can be presented in a 1-D or 2-D format. InSAR measures surface displacement on a one-dimensional plane, along the satellite line-of-sight. Data can be collected from either the ascending orbit or the descending orbit. The line-of-sight angles can vary. Ascending satellites travel from south to north while imaging to the east, whereas descending satellites travel from north to south and image to the west. By combining results from the two acquisition geometries a true vertical displacement and east-west horizontal displacement can be derived, known as a two-dimensional movement analysis.

The current set of 2-D data was delivered November 2018 by TRE Altamira and reports on the continued collection of radar imagery from two different satellite orbits acquired over the timeline, presented in Figure 10 and Table 2. The imagery has been collected from the TerraSAR-X (TSX)

satellite. Fewer images were acquired from the descending orbit, because the satellite was re-directed for another mission.

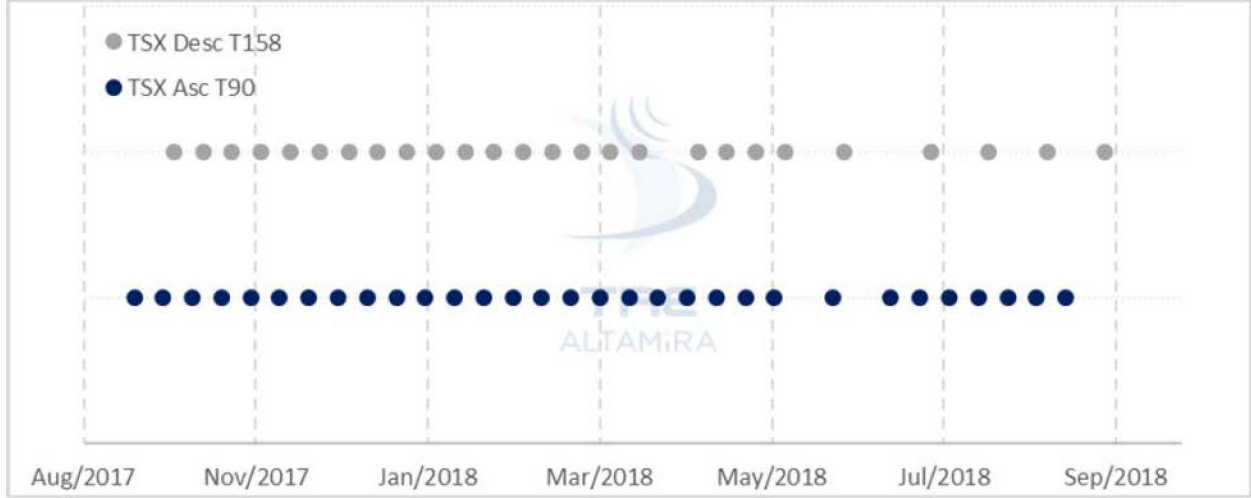


Figure 10. Time period covered by satellite data sets [13].

Table 2. 2-D InSAR data sets

| Satellite | Geometry | No. of Images | Number of Measurement Points | Repeat Interval | Acquisition Period |
|-----------|------------|---------------|------------------------------|-----------------|-----------------------|
| TSX | Ascending | 31 | 15,306 | 11-days | 09/16/2017-09/03/2018 |
| TSX | Descending | 26 | 11,852 | 11-days | 10/01/2017-09/18/2018 |

4.2.1. Line of Sight Results

Figure 11 displays the results from both the ascending and descending geometries. The reference location was selected from an area of stable measurements, in this instance located along the north-south road to the west of the salt dome. The look direction for the ascending acquisition was collected at an angle of 17.5° , whereas the descending look angle was at 54.7° . It is apparent that the results from both acquisition geometries are not identical. More vertical angles will be more sensitive to vertical movement, whereas higher angles will be more sensitive to horizontal motion. The average surface deformation rate calculated from the ascending data is -0.37 ± 0.06 in/yr. (-9.3 ± 1.5 mm/yr.). The descending results are -0.12 ± 0.06 in/yr. (-3.0 ± 1.6 mm/yr.). The 2D analysis takes both data sets, that can appear different, decomposes the results, and provides a true vertical and east-west horizontal displacement measurements.

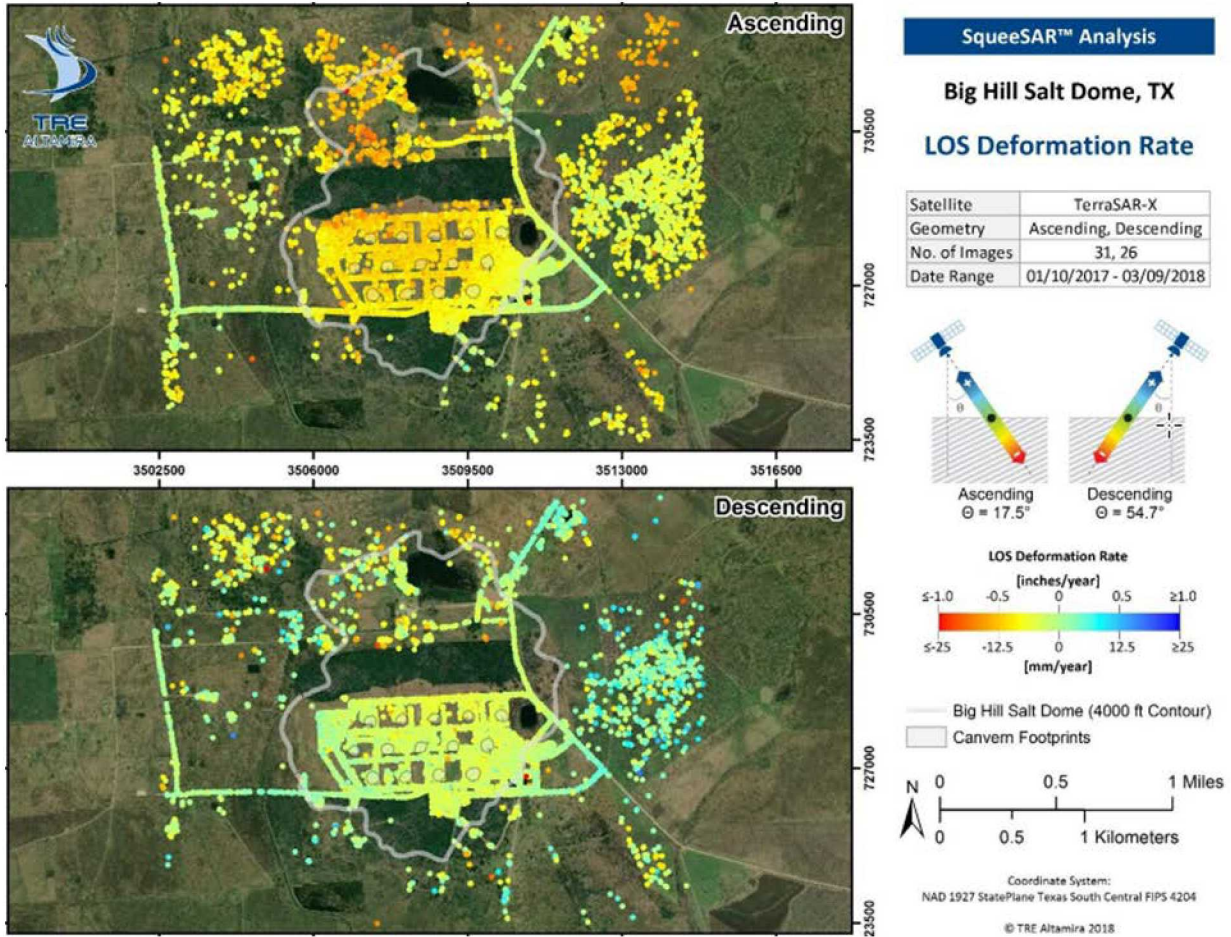


Figure 11. Annual surface displacement rates obtained from the ascending and descending InSAR analysis [13].

4.2.2. 2D Results

4.2.2.1. Vertical Surface Displacement

The decomposed vertical displacement rates are displayed in Figure 12. In general, the average displacement rate is -0.31 ± 0.05 in/yr. (-7.8 ± 1.2 mm/yr.) The trend shows minimal movement along the off-site roads, suggesting stability, and general increase in subsidence towards the middle of the site and salt dome. The greatest subsidence is centered over caverns 103 and 104, located at the north central region of the Big Hill site, where the subsidence is -0.65 in/yr. (-16.4 mm/yr.). Upward movement is noted towards the east off the salt dome ($+0.17$ in/yr., $+4.3$ mm/yr.). No uplift was noted over the Big Hill site.

As was done with historic data, the current vertical results were split into subsets, to aid in visualizing the surface behavior across the dome in more depth. The time series were averaged for each subset from both west to east and from north to south (Figure 13 and Figure 14). Subsidence is greatest in the north and decreases in rate towards the south. From the west to east subsidence is greatest over the center of the site, with the western portion subsiding at a faster rate when compared the eastern region. This closer look supports the previous conclusions that the greatest subsidence is occurring over the north central region of the site.

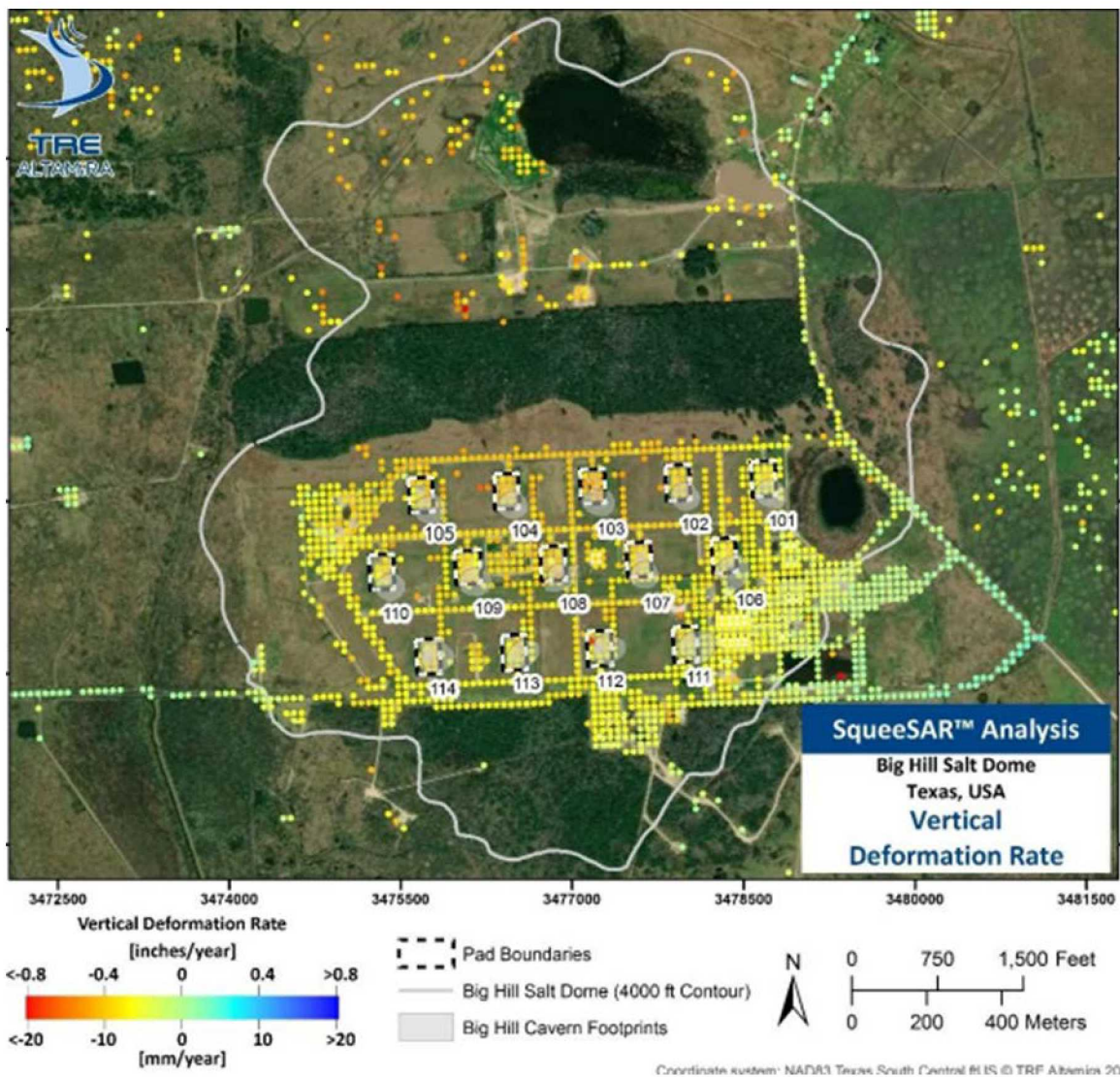


Figure 12. Surface displacement results obtained from the vertical 2-D InSAR analysis [13].

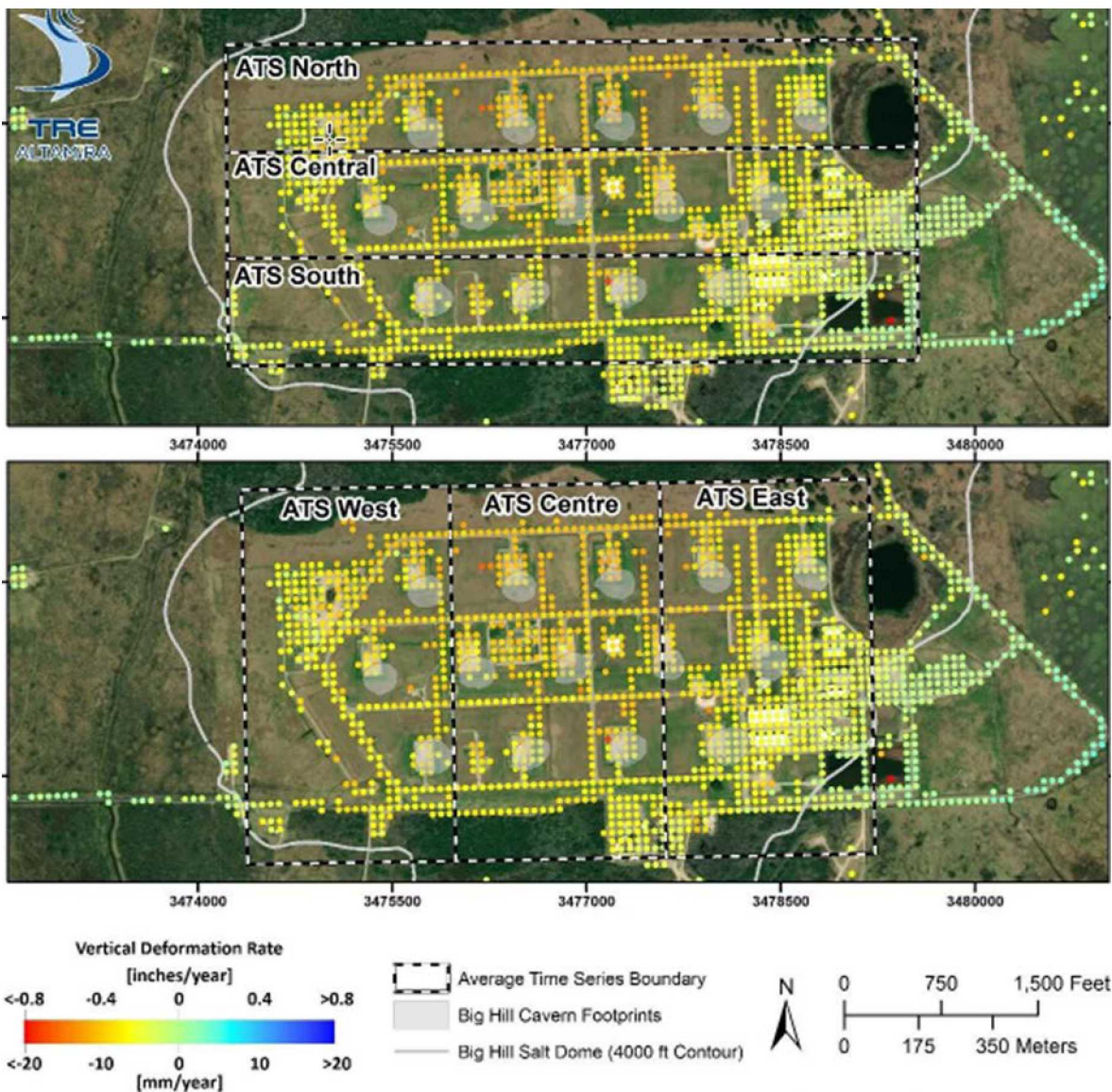


Figure 13. Vertical deformation rate with six areas highlighted for average time series [13].

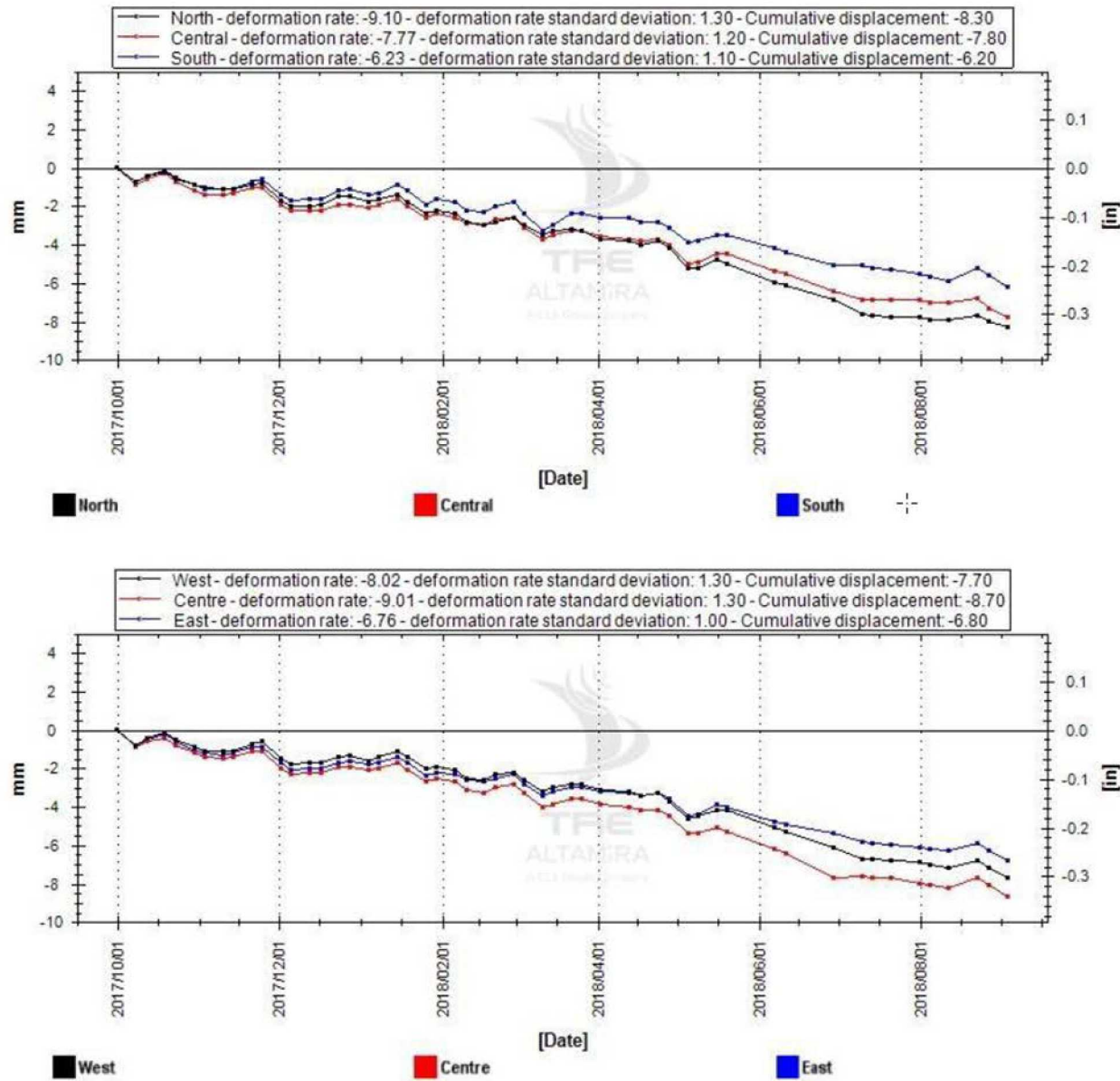


Figure 14. Average time series of the six regions highlighted in Figure 13 [13].

In addition to analyzing multiple polygon regions across the site, three surface profiles were examined to look at change over time. The locations are delineated in Figure 15.

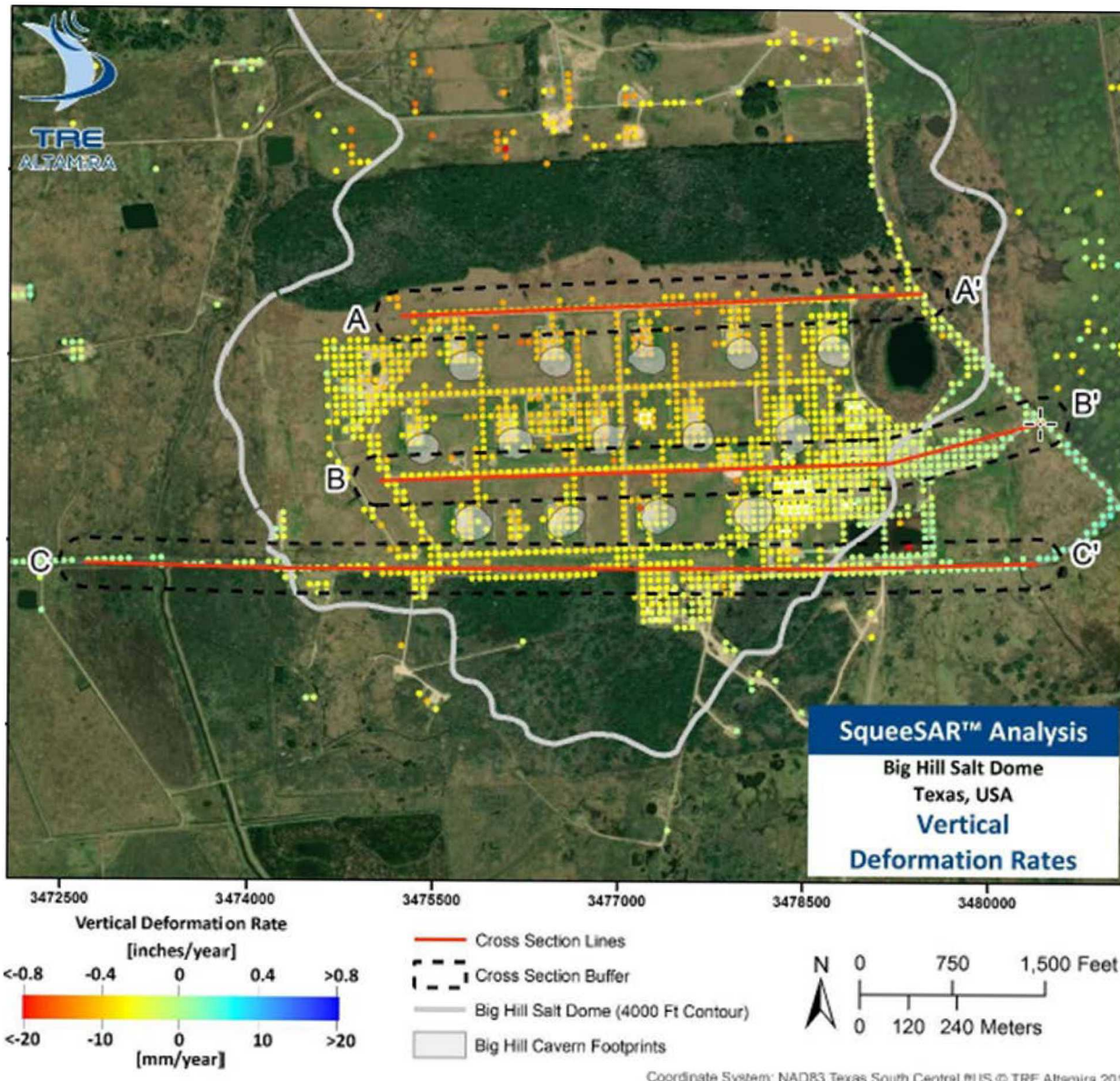


Figure 15. Trace of the cross-section lines over the salt dome. Vertical cross sections are shown in Figure 16 to Figure 18 [13].

Cross section A-A' exhibits near linear subsidence (Figure 16). Slope changes and subsidence slows east of the last cavern (Cavern 101).

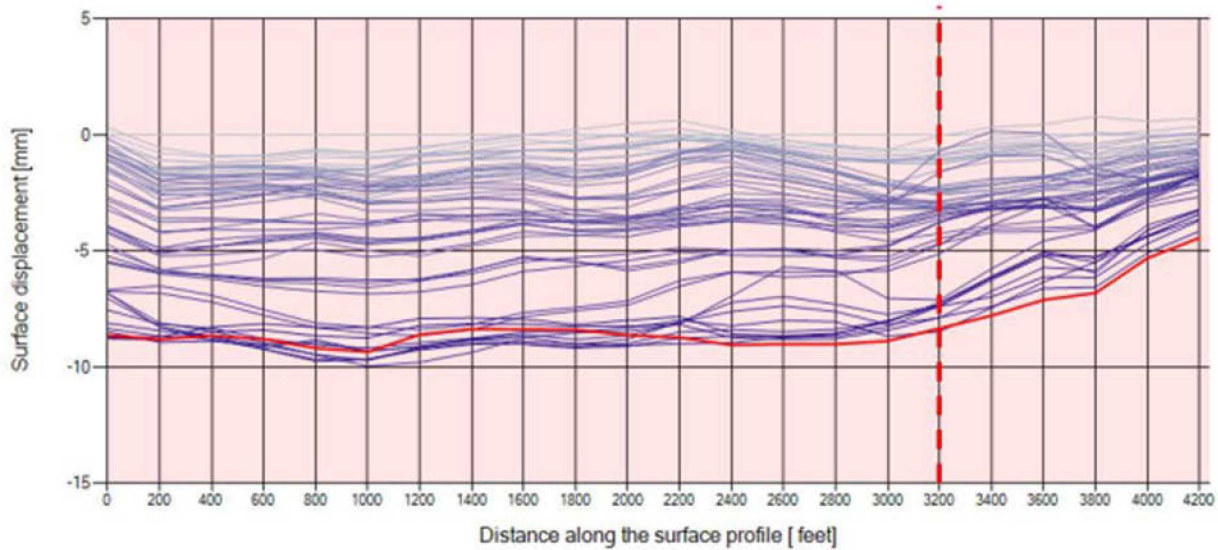


Figure 16. Evolution of the surface profile cross section A – A'. The solid profile highlighted in red corresponds to the final image of the data stack. The dashed vertical line in red corresponds to the location on the profile line where the elevation of salt changes (1650-feet) [13].

Cross section B-B' (Figure 17) indicates the greatest subsidence is occurring towards middle of site between caverns 107 and 108. Surface displacement is less towards both the west and east directions. As noted previously, the subsidence is greater over the western side of the site when compared to the east. The surface deformation, past the edge of the top-of-salt, decreases and eventually begins to uplift well off the dome.

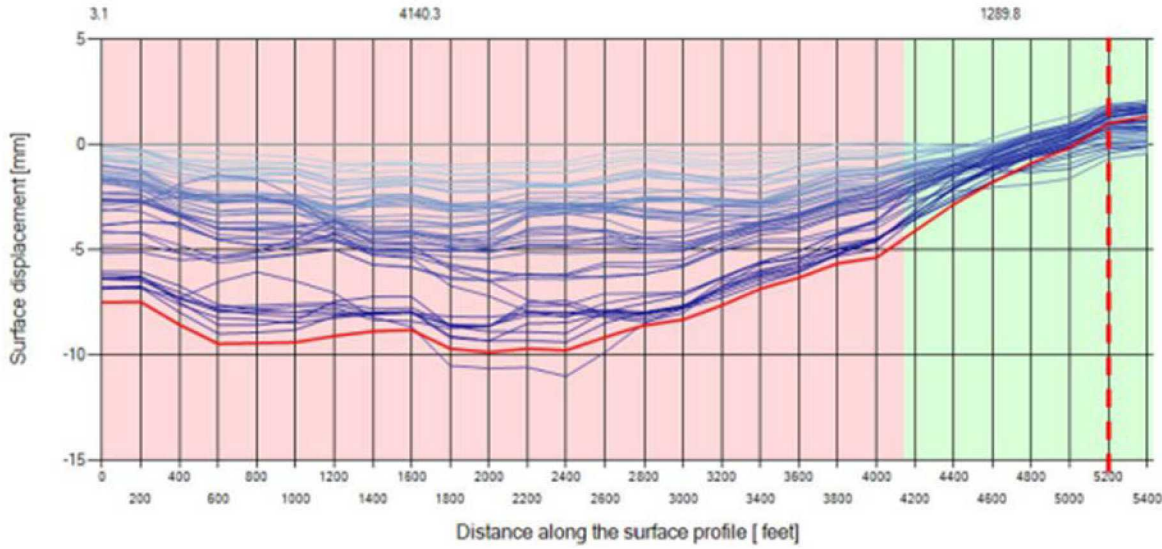


Figure 17. Evolution of the surface profile cross section B – B'. The solid profile highlighted in red corresponds to the final image of the data stack. The contrasting background colors (pink/green) illustrate where the profile crosses the 4000-ft salt contour, while the dashed vertical line in red corresponds to the edge of the salt dome on the profile line [13].

Cross section C-C' (Figure 18) displays near linear subsidence across the dome. Subsidence character changes past the dome edge and suggests surface stability towards the west and surface uplift towards the east.

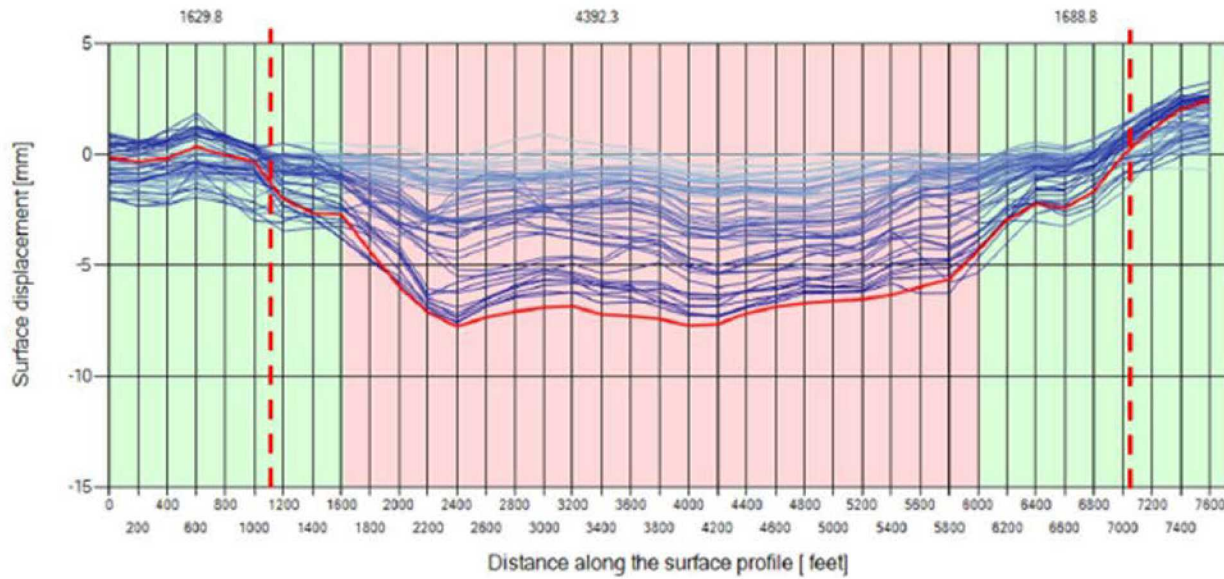


Figure 18. Evolution of the surface profile cross section C – C'. The solid profile highlighted in red corresponds to the final image of the data stack. The contrasting background colors (pink/green) illustrate where the profile crosses the 4000-ft salt contour, while the dashed vertical lines in red corresponds to the edge of the salt dome on the profile line [13].

4.2.2.2. Horizontal Surface Displacement

The decomposed east-west horizontal rates are displayed in Figure 19. Overall the horizontal motion is towards the center of the Big Hill site. A stronger eastward motion is noted from the western portion of the site. Overall, horizontal motion is minimal, and the rate average is -0.06 ± 0.06 in/yr. (-1.5 ± 1.6 mm/yr.). Motion towards the east, from the west side, is -0.37 in/yr. ($+9.4$ mm/yr.); westward motion noted from the eastern side is -0.21 in/yr. (-5.4 mm/yr.). Strongest horizontal movement seen over the caverns is measured at caverns 114 and 110. The horizontal trend observed matches the development of the subsidence bowl seen from the analysis of the vertical decomposed data.

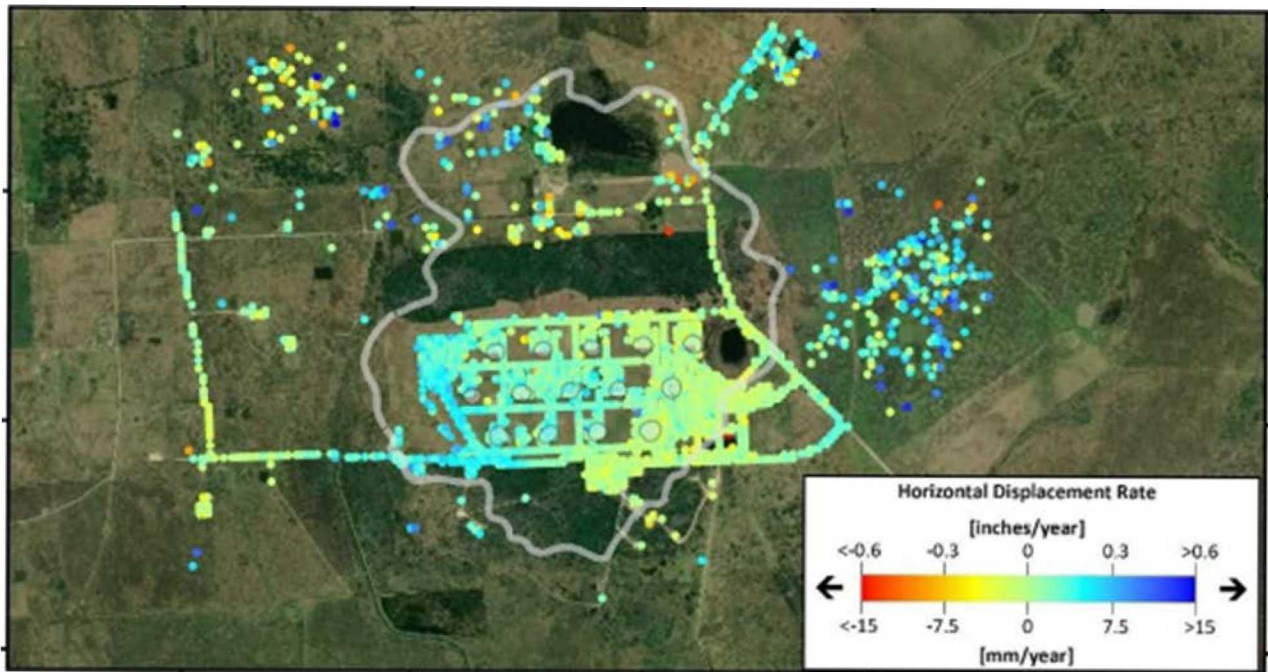


Figure 19. Horizontal east-west surface displacement results obtained from the 2D InSAR analysis [13].

5. DISCUSSION

Comparison between the three data sets is challenging. All are different data, designed differently, with various time frames, some measuring regions versus single points with different sampling density. With all that being said, the survey types show the same surface pattern, essentially a subsidence bowl centered across the Big Hill cavern site. Highest subsidence is observed in the center of the site, and the least subsidence is on the edge of the site. This is the general trend expected to be exhibited over a cavern field. The differences highlighted between data sets questions whether surface uplift is occurring over the site. All three datasets record some degree of uplift, albeit over different locations dependent on the data set. The ground surveys, since 2002, are indicating uplift is occurring over both the western and eastern portions of the Big Hill property and cavern field. The historic InSAR suggests the rate of subsidence slowed during 2009 and uplift was noted over the western portion of the site. The current InSAR data acquired over the last year suggests minor uplift is occurring off the dome to the east. The current average rate is similar to the historic rate, before the shift occurred in 2009, suggesting the rate has resumed.

In investigating the validity of the uplift measured during the ground surveys it was discovered that reference location can impact results. An exercise was conducted that took the current InSAR data and presented two varying results dependent on the reference location, either on or off the dome. The two different sets of results are shown in Figure 20. The conclusion was that if the reference is located on the dome, as it has been for years for the ground surveys, the reference location is moving too, giving the appearance of uplift. In 2018 new reference locations were established off the dome for the ground surveys. The latest ground survey data was just received by Sandia and the preliminary analysis of the results (Figure 21) resemble the current InSAR analysis, supporting that the perceived surface uplift was an artifact of the reference benchmark being located on the dome.

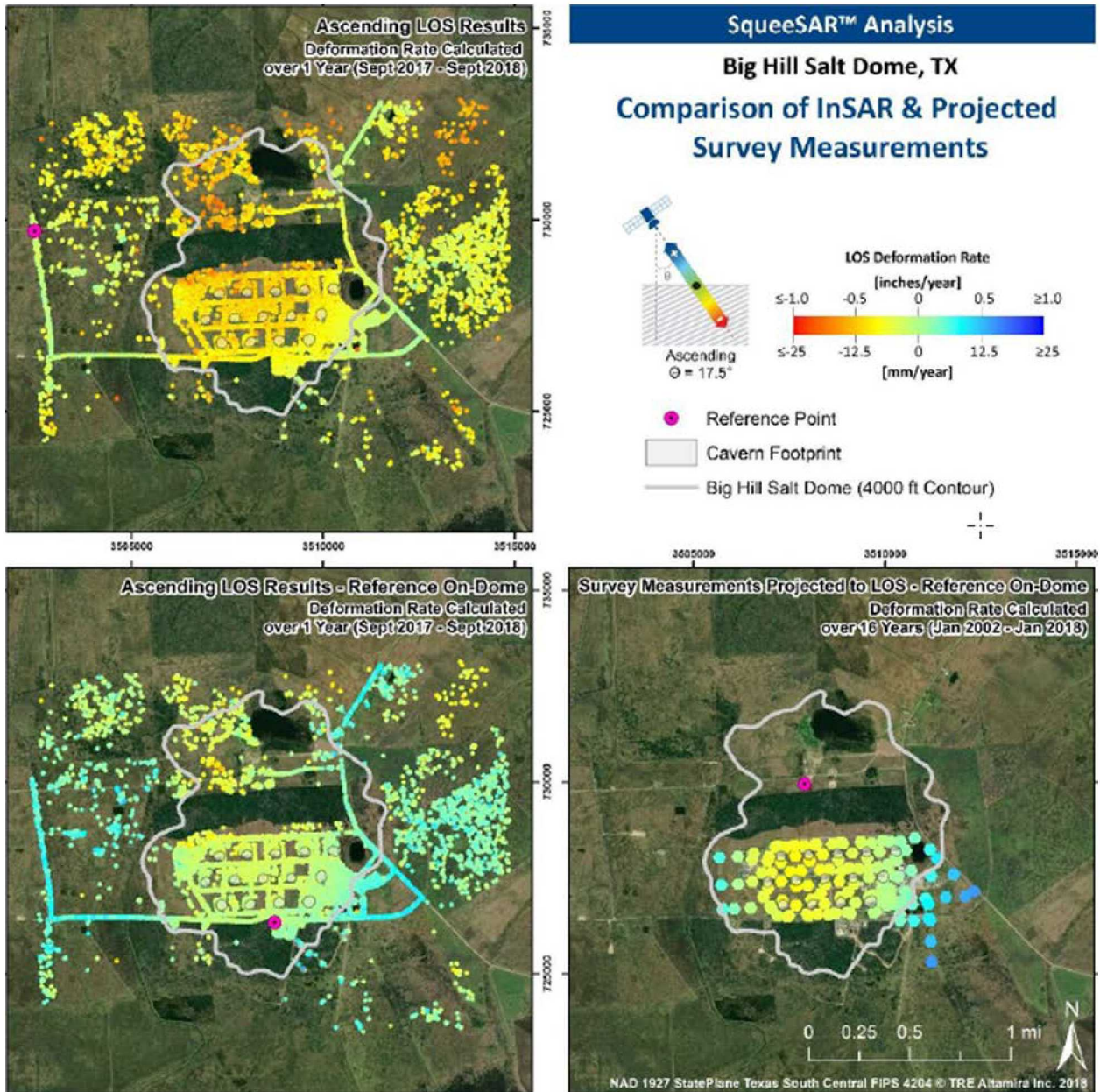


Figure 20. Comparison of deformation rates obtained from the ascending InSAR results and ground-based surveys. Top left: Deformation rates obtained from the ascending InSAR analysis; Bottom right: Deformation rates calculated from ground-based survey measurements projected to satellite's line of site angle. Note that the network's reference point exhibits subsidence within InSAR results; Bottom left: Deformation rates obtained from the ascending InSAR analysis using a reference on the dome with known subsidence issues [13].

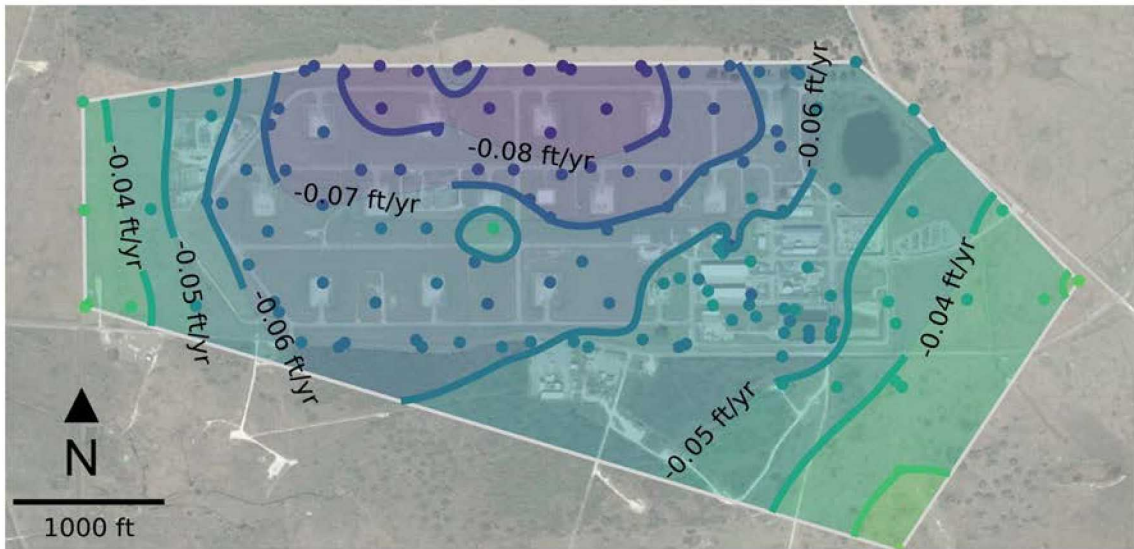


Figure 21. Big Hill subsidence rates, January 2018 to January 2019.

We are potentially now just starting to understand the actual subsidence behavior, with both the inclusion of temporal frequency and point density data collection and the establishment of reference benchmarks located off dome. Once we can establish a pattern and trend that is defendable, we will be able to understand the mechanism causing the surface deformation, such as response from cavern depressurization as seen in previous years and at other sites.

The 2-D analysis indicates the fastest subsidence rates are over the north central region of the site, specifically centered over caverns 104 and 103. Subsidence rates decrease towards both the west and east, with the western side subsiding at greater rate than the eastern edge. There is some uplift noted, off the site and off the dome to the east. Overall, the subsidence pattern is in line with subsidence behavior expected over a cavern field.

In summary, InSAR technology provides the benefit of providing increased temporal frequency and point density data collection when compared to the current level-and-rod survey method. Satellite images are collected every 11 days compared to a ground survey shot once a year. With the continued collection of more images over a longer temporal period both the point density and precision will continue to improve. What the InSAR technology provides, which cannot be duplicated by the ground surveys, is a continuous stream of data, which provides confidence that the surface deformation behavior is true (e.g. is the ground surface uplifting?).

InSAR images are continuing to be collected, from the two different geometries, over the Big Hill site through October 2019. The next analysis report to be provided by TRE Altamira will be delivered November 2019.

REFERENCES

- [1] Lord, A. S. 2013. May 2013 Big Hill Subsidence Analysis, letter report submitted to P. Tilly DOE PMO, February 25, 2014.
- [2] Lord, A. S. 2012. May 2012 Big Hill Subsidence Analysis, letter report submitted to P. Tilly DOE PMO, November 15, 2012.
- [3] Lord, A. S. 2009. February 2009 Big Hill Subsidence Analysis, letter report submitted to W. Elias, DOE PMO, April 15, 2009.
- [4] Ehgartner, B. and S. Bauer. 2004. Large Scale Salt Deformation: Comments on subsidence using thermal, creep and dissolution modeling to assess volumetric strain. Solution Mining Research Institute, Spring Meeting, Wichita, KS, 2004.
- [5] Magorian, T. R. and J. T. Neal. 1988. Strategic Petroleum Reserve (SPR) Additional Geolgoical Site Characterization Studies, Big Hill Salt Dome, Texas. Sandia Report SAND88-2267. Sandia National Laboratories, Albuquerque, NM.
- [6] Neal, J. T., Magorian, T. R., Thoms, R. L., Autin, W. J., McCulloh, R. P., Denzler, S., and Byrne, K. O. 1993. Anomalous Zones in Gulf Coast Salt Domes with Special Reference to Big Hill, TX, and Weeks Island, LA. Sandia Report SAND92-2283. Sandia National Laboratories, Albuquerque, NM.
- [7] Lord, A. S., Sobolik, S.R., and B.L. Roberts. 2015. Understanding the Big Hill Dome Surface Uplift: Historical InSAR Study. Solution Mining Research Institute, Fall Meeting, Santander, Spain, 2015
- [8] Lord, A.S. 2013. Holistic Understanding of the Big Hill Salt Dome Geologic Processes in Relation to Impacts on Cavern Well Integrity. Solution Mining Research Institute, Spring Meeting, Lafayette, LA, 2013.
- [9] Lord, A.S. and C. L. Kirby. 2013. Impact of Waste Injection Wells on Big Hill Subsidence, letter report submitted to P. Tilly, DOE PMO, July 10, 2013.
- [10] Moriarty, D. 2017. August 2016 Big Hill Subsidence Report, letter report to D. Willard, DOE PMO, June 20, 2017.
- [11] Moriarty, D. 2018. July 2017 & January 2018 Big Hill Subsidence Report, letter report to D. Willard, DOE PMO, May 31, 2018.
- [12] CGG. 2014. Technical Report: Big Hill Historical InSAR Study. August 19, 2014.
- [13] TRE Altamira. 2018. 2D SqueeSAR Analysis of Ground Movement Over Big Hill Salt Dome. Report JO17-369-CA. November 6, 2018.

DISTRIBUTION

Email—External (encrypt for OUO)

| Name | Company Email Address | Company Name |
|--------------------------|--------------------------------------|-----------------------------------|
| Wayne Elias | Wayne.elieas@hq.doe.gov | DOE SPR Program Office |
| James Gruber | James.gruber@hq.doe.gov | DOE SPR Program Office |
| Claudia LeCompte-Johnson | Claudia.lecompte-johnson@spr.doe.gov | DOE SPR Project Management Office |
| Paul Malphurs | Paul.malphurs@spr.doe.gov | DOE SPR Project Management Office |
| Diane Willard | Diane.willard@spr.doe.gov | DOE SPR Project Management Office |

Email—Internal

| Name | Org. | Sandia Email Address |
|-------------------|-------|--|
| Erik Webb | 8860 | ekwebb@sandia.gov |
| Donald Conley | 8862 | dconley@sandia.gov |
| Carolyn Kirby | 8862 | clkirby@sandia.gov |
| Dylan Moriarty | 8862 | dmmoria@sandia.gov |
| Technical Library | 01177 | libref@sandia.gov |

This page left blank

This page left blank



**Sandia
National
Laboratories**

Sandia National Laboratories is a multimission laboratory managed and operated by National Technology & Engineering Solutions of Sandia LLC, a wholly owned subsidiary of Honeywell International Inc. for the U.S. Department of Energy's National Nuclear Security Administration under contract DE-NA0003525.